Abstracts

CATALYSIS – APPLIED AND PHYSICAL ASPECTS

Studies on the Catalytic Ability of Palladium Wire, Foil and Sponge in the Suzuki–Miyaura Cross-Coupling

F. Amoroso, U. Cersosimo and A. Del Zotto, *Inorg. Chim. Acta*, 2011, **375**, (1), 256–262

Different forms of metallic Pd were evaluated in the Suzuki-Miyaura cross-coupling reaction. All samples were found to be catalytically active for both electron-poor and electron-rich aryl bromides combined with a variety of arylboronic acids. Pd wire was recycled six times without decrease of catalytic activity. A series of poisoning experiments demonstrated that the true catalyst is a soluble form of Pd arising from a leaching process.

Investigation of Heterogeneous Asymmetric Dihydroxylation over OsO_4–$(QN)_2PHAL$ Catalysts of Functionalized Bimodal Mesoporous Silica with Ionic Liquid

S. Qiu, J. Sun, Y. Li and L. Gao, *Mater. Res. Bull.*, 2011, **46**, (8), 1197–1201

1-Methyl-3-(trimethoxysilyl)propylimidazolium chloride was grafted onto the surface of bimodal mesoporous silicas (BMMs), and then 1,4-bis(9-*O*-quininyl)-phthalazine ($(QN)_2$-PHAL) and $K_2Os(OH)_4{\cdot}2H_2O$ were immobilised onto the resulting functionalised bimodal mesoporous silica with ionic liquid (FBMMs) by adsorption or ionic exchange. The mesoporous ordering degree of the bimodal mesoporous silica decreased after functionalisation and immobilisation of OsO_4-$(QN)_2$PHAL. The solid catalyst was effective in asymmetric dihydroxylation with high yield and enantioselectivity, and could be recycled for five times.

CATALYSIS – REACTIONS

A Continuous-Flow Approach to Palladium-Catalyzed Alkoxycarbonylation Reactions

C. B. Kelly, C. (X.) Lee, M. A. Mercadante and N. E. Leadbeater, *Org. Process Res. Dev.*, 2011, **15**, (3), 717–720

Using a continuous-flow approach, alkoxycarbonylations of aryl iodides were performed using $Pd(OAc)_2$ (0.5 mol%) as catalyst with no additional ligand. Optimised reactor design allowed for adequate mixing of the gaseous and liquid reagents. Reactions were performed at rates of ~3 ml min^{-1} and at concentrations of 1 M, allowing for significant volumes to be processed per unit time.

Borrowing Hydrogen Methodology for Amine Synthesis under Solvent-Free Microwave Conditions

A. J. A. Watson, A. C. Maxwell and J. M. J. Williams, *J. Org. Chem.*, 2011, **76**, (7), 2328–2331

Microwave heating was applied to the 'borrowing hydrogen strategy' to form C–N bonds from alcohols and amines, removing the need for solvent and reducing reaction times. For example, DPEphos, $[Ru(p\text{-cymene})Cl_2]_2$, benzyl alcohol and morpholine were added to a microwave vial containing a stirrer bar.

A. J. A. Watson *et al.*, *J. Org. Chem.*, 2011, **76**, (7), 2328–2331

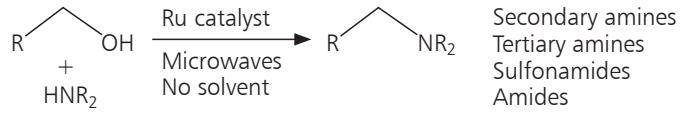

The vial was then sealed before purging with N_2 for 5 min. The reaction was then heated to 115°C for 90 min using a microwave. The crude material was then purified to give *N*-benzylmorpholine.

EMISSIONS CONTROL

Photocatalytic Membrane Contactors for Water Treatment

I. Kumakiri, S. Diplas, C. Simon and P. Nowak, *Ind. Eng. Chem. Res.*, 2011, **50**, (10), 6000–6008

Commercial TiO_2 particles (P25 and ST01) were deposited on porous ceramic materials. Pt was then deposited from a H_2PtCl_6 aqueous solution onto TiO_2 by the photoreduction method. The activity of the resulting three-phase photocatalytic membrane contactor (CMC) was studied for the removal of model contaminants such as formic, oxalic and humic acids from water. The highest degradation rate was observed under UV irradiation with simultaneous O_2 supply. The catalytic activity was maintained during several months of testing and several months of storage in air.

FUEL CELLS

A Study of the Methane Tolerance of LSCM–YSZ Composite Anodes with Pt, Ni, Pd and Ceria Catalysts

J.-S. Kim, V. V. Nair, J. M. Vohs and R. J. Gorte, *Scr. Mater.*, 2011, **65**, (2), 90–95

The performance of SOFC anodes based on composites of LSCM and YSZ containing 0.5 wt% metal catalyst was studied. Electrodes containing Pt were stable in CH_4 but C deposits with granular or filamentous morphologies were found with electrodes containing either 0.5 wt% Pd or Ni. C deposition with both Pd and Ni was suppressed by the addition of 10 wt% ceria as a cocatalyst.

Activity, Stability, and Degradation Mechanisms of Dealloyed $PtCu_3$ and $PtCo_3$ Nanoparticle Fuel Cell Catalysts

F. Hasché, M. Oezaslan and P. Strasser, *ChemCatChem*, 2011, **3**, (11), 1805–1813

A stability and activity study of supported dealloyed $PtCu_3$ and $PtCo_3$ NP catalysts for the ORR was carried out. $PtCu_3$ and $PtCo_3$ were subjected to two voltage cycling tests: a 'lifetime' regime (10,000 cycles, 0.5–1.0 V *vs.* RHE, 50 mV s^{-1}) and a corrosive 'start-up' regime (2000 cycles, 0.5–1.5 V *vs.* RHE, 50 mV s^{-1}). Significant activity and stability benefits were demonstrated for dealloyed $PtCu_3$ and $PtCo_3$ for the ORR compared with those of pure Pt. After testing in the 'lifetime' regime, the Pt-surface-area-based activity of the Pt alloy catalysts was still twice as high as that of pure Pt.

Pt–Ru Alloyed Fuel Cell Catalysts Sputtered from a Single Alloyed Target

A. A. Dameron, T. S. Olson, S. T. Christensen, J. E. Leisch, K. E. Hurst, S. Pylypenko, J. B. Bult, D. S. Ginley, R. P. O'Hayre, H. N. Dinh and T. Gennett, *ACS Catal.*, 2011, **1**, (10), 1307–1315

$Pt_{1-x}Ru_x$ NPs with compositions from $Pt_{0.32}Ru_{0.68}$ to $Pt_{0.50}Ru_{0.50}$ were sputtered from a single alloyed target to deposit on the surface of a C matrix support. The control of parameters such as sputter gas type, sputter gas concentration, deposition pressure, sputter power, and sputter type (RF or DC) resulted in a low metal loading catalyst, ~30 wt%, with a MeOH oxidation reaction onset potential of <300 mV *vs.* RHE and peak current of >200 μA cm^{-2}. The optimised catalysts outperformed commercially available catalysts at DMFC operating potentials.

METALLURGY AND MATERIALS

Surface Geometry of Pure Iridium Oxidized at 1373 K in Air

Z. B. Bao, H. Murakami and Y. Yamabe-Mitarai, *Appl. Surf. Sci.*, 2011, **258**, (4), 1514–1518

The surface microstructure of a polished Ir sample during isothermal heat treatment at 1373 K in air exhibited triangular pits and terraces, 'pyramid'-like plateaus and striated edges. The changes in surface geometry were dependent on the original grain orientation. Most grains were confirmed to possess or partly exhibit a geometric configuration of {1 1 1} faceting habit, while periodic bond chain vectors played an important role in determining the ultimate surface morphology.

Effect of Ruthenium on High-Temperature Creep Rupture Life of a Single Crystal Nickel-Based Superalloy

X. P. Tan, J. L. Liu, T. Jin, Z. Q. Hu, H. U. Hong, B. G. Choi, I. S. Kim and C. Y. Jo, *Mater. Sci. Eng.: A*, 2011, **528**, (29–30), 8381–8388

The addition of 3 wt% Ru improved the creep rupture lives of a single crystal Ni-based superalloy at 1100°C/150 MPa and 1000°C/310 MPa. The change of γ/γ′ lattice misfit in the initial microstructure is believed to be the key role of Ru on the high-temperature creep deformation. The larger negative lattice misfit caused by the addition of Ru induces smaller and more regular γ′ particles in the initial state, as well as denser dislocation networks at the γ/γ′ interface during creep.

CHEMISTRY

Hydrogenolysis of Palladium(II) Hydroxide, Phenoxide, and Alkoxide Complexes

G. R. Fulmer, A. N. Herndon, W. Kaminsky, R. A. Kemp and K. I. Goldberg, *J. Am. Chem. Soc.*, 2011, **133**, (44), 17713–17726

($^{t\mathrm{Bu}}$PCP)Pd(II)–OR ($^{t\mathrm{Bu}}$PCP = 2,6-bis($CH_2P^tBu_2$)C_6H_3; R = H, CH_3, C_6H_5, $CH_2C(CH_3)_3$, CH_2CH_2F, CH_2CHF_2 or CH_2CF_3) pincer complexes were synthesised. Hydrogenolysis of the Pd hydroxide complex to generate the Pd hydride complex and H_2O was inhibited by formation of a water-bridged, H-bonded Pd(II) hydroxide dimer. The Pd alkoxide and aryloxide complexes exhibited reactivity dependent on the –OR ligand (steric bulk, electron-donating ability, and/or the presence of β-hydrogen atoms). Full selectivity for hydrogenolysis was observed with the Pd(II) 2-fluoroethoxide complex.

G. R. Fulmer *et al.*, *J. Am. Chem. Soc.*, 2011, **133**, (44), 17713–17726

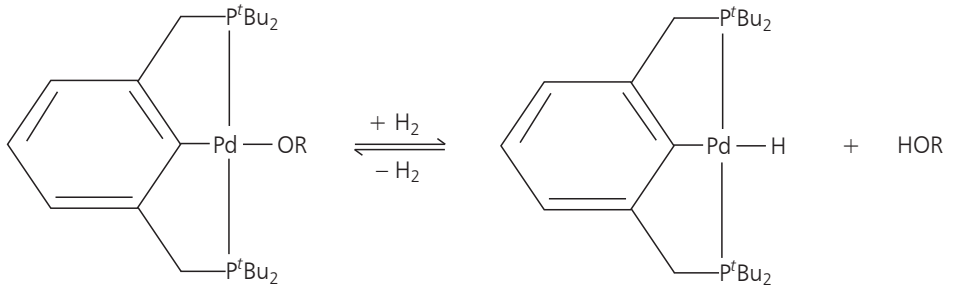

R = H, CH_3, C_6H_5, $CH_2C(CH_3)_3$, CH_2CH_2F, CH_2CHF_2, CH_2CF_3

ELECTRICAL AND ELECTRONICS

Optimization of $L1_0$-FePt/MgO/CrRu Thin Films for Next-Generation Magnetic Recording Media

R. Fernandez, N. Amos, C. Zhang, B. Lee and S. Khizroev, *Thin Solid Films*, 2011, **519**, (22), 8053–8057

$L1_0$-FePt thin films were deposited on Si substrates with the structure Si/CrRu/MgO/FePt. The magnetic and microstructural properties were optimised by varying the FePt sputter pressure and temperature, as well as the thicknesses of all three layers. High coercivity thin films greater than 1.8 T were obtained when the FePt sputter pressure was 1.33 Pa with a thickness of 4 nm, on CrRu and MgO underlayers of 10 nm and 2 nm, respectively.

MEDICAL AND DENTAL

Organometallic Iridium(III) Cyclopentadienyl Anticancer Complexes Containing C,N-Chelating Ligands

Z. Liu, A. Habtemariam, A. M. Pizarro, G. J. Clarkson and P. J. Sadler, *Organometallics*, 2011, **30**, (17), 4702–4710

$[(\eta^5\text{-}Cp^x)Ir(C\text{^}N)Cl]$ (Cp^x = Cp*, C^N = 2-(*p*-tolyl)pyridine (**1**), 2-phenylquinoline (**2**), 2-(2,4-difluorophenyl)-pyridine (**3**); Cp^x = tetramethyl(phenyl)cyclopentadienyl (Cp^{xph}), C^N = 2-phenylpyridine (**4**); and Cp^x = tetramethyl(biphenyl)cyclopentadienyl (Cp^{xbiph}), C^N = 2-phenylpyridine (**5**)) have been synthesised and characterised. **2** and **5** have typical 'piano-stool' geometry. All the complexes hydrolysed rapidly in aqueous solution (<5 min). All the complexes showed potent cytotoxicity, with IC_{50} values from 6.5 to 0.7 μM toward A2780 human ovarian cancer cells. Potency increased with additional phenyl substitution on Cp*: $Cp^{xbiph} > Cp^{xph} > Cp^*$. Cp^{xbiph} with **5** exhibited submicromolar activity (twice as active as cisplatin).

$[Ru(bpy)_2(5\text{-cyanouracil})_2]^{2+}$ as a Potential Light-Activated Dual-Action Therapeutic Agent

R. N. Garner, J. C. Gallucci, K. R. Dunbar and C. Turro, *Inorg. Chem.*, 2011, **50**, (19), 9213–9215

cis-$[Ru(bpy)_2(5CNU)_2]^{2+}$ (5CNU = 5-cyanouracil) was shown to undergo efficient photoinduced 5CNU ligand exchange for solvent H_2O molecules, thus simultaneously releasing biologically active 5CNU and generating $[Ru(bpy)_2(H_2O)_2]^{2+}$. The latter binds covalently to double-stranded DNA, such that photolysis results in the generation of 3 equiv. of potential therapeutic agents from a single molecule.

NANOTECHNOLOGY

Patchy Multishell Segregation in Pd–Pt Alloy Nanoparticles

G. Barcaro, A. Fortunelli, M. Polak and L. Rubinovich, *Nano Lett.*, 2011, **11**, (4), 1766–1769

Chemical ordering in fcc-like PdPt NPs consisting of 38–201 atoms was studied *via* DFT calculations combined with a symmetry orbit approach. It was found that for larger particles in the Pd-rich regime, Pt atoms could segregate at the centre of the NP (111) surface facets, in contrast with extended systems in which Pd is known to segregate at the surface of alloy planar surfaces. In a range of compositions around 1:1, a novel multishell chemical ordering pattern was favoured, in which each shell is a patchwork of islands of atoms of the two elements, but the order of the patchwork was reversed in the alternating shells.